1521-0103/12/3411-156–163$25.00
THE JOURNAL OF PHARMACOLOGY AND EXPERIMENTAL THERAPEUTICS
Vol. 341, No. 1
189050/3756691
JPET 341:156–163, 2012

A Humanized Glycoprotein VI (GPVI) Mouse Model to Assess the Antithrombotic Efficacies of Anti-GPVI Agents[S]

Pierre Henri Mangin, ChaoJun Tang, Catherine Bourdon, Stéphane Loyau, Monique Freund, Béatrice Hechler, Christian Gachet, and Martine Jandrot-Perrus

Unité Mixte de Recherche Scientifique 949, Institut National de la Santé et de la Recherche Médicale, Strasbourg, France (P.H.M., C.T., C.B., M.F., B.H., C.G.); Université de Strasbourg, Strasbourg, France (P.H.M., C.T., C.B., M.F., B.H., C.G.); Etablissement Français du Sang-Alsace, Strasbourg, France (P.H.M., C.T., C.B., M.F., B.H., C.G.); Unité Mixte de Recherche Scientifique 698, Institut National de la Santé et de la Recherche Médicale, Paris, France (S.L., M.J.-P.); Université Paris 7, Paris, France (S.L., M.J.-P.); and Hôpital Xavier Bichat, Assistance Publique Hôpitaux de Paris, Paris, France (S.L., M.J.-P.)

Received October 14, 2011; accepted January 9, 2012

ABSTRACT

Glycoprotein VI (GPVI) has been proposed as a promising antiplatelet target, because its blockade prevents experimental thrombosis without impairing hemostasis. The objective of this study was to develop a preclinical tool to evaluate the role of human GPVI (hGPVI) in various models of thrombosis and to screen anti-GPVI compounds. A genetically modified mouse strain expressing hGPVI has been developed using a knockin strategy. The mice were viable and fertile and did not present any hematological defects. Approximately 3700 copies of human GPVI were detected at the platelet surface. Platelet aggregation, fibrinogen binding, and P-selectin exposure were normal in response to various agonists. The 9O12.2 Fab fragment directed against human GPVI bound to hGPVI platelets in vitro and ex vivo and markedly reduced collagen- and collagen-related peptide-induced responses. Injection of 9O12.2 into hGPVI animals did not prolong the tail bleeding time but provided protection against lethal thromboembolism induced by a collagen/adrenaline mixture. In addition, 9O12.2 reduced arterial thrombus growth by 44% after superficial laser injury, 43% after deep laser injury in mice pretreated with hirudin, and 48% after mechanical injury. In conclusion, we have developed a humanized mouse model that could be used in preclinical studies to evaluate the effects of anti-GPVI compounds.

Introduction

The treatment of acute coronary syndromes has been improved considerably in recent years with the introduction of highly efficient antiplatelet drugs, the current standard treatment being based on dual antiplatelet therapy with aspirin and a thienopyridine. However, this strategy still has significant limitations: the recurrence of adverse vascular events remains a problem, and the improvement in efficacy is counterbalanced by an increased risk of bleeding. The search for better antiplatelet drugs that efficiently prevent platelet thrombus formation while having a minimal effect on general hemostasis remains a competitive challenge (Jackson and Schoenwaelder, 2003; Yousuf and Bhatt, 2011).

Glycoprotein VI (GPVI) is considered to be an attractive target for the development of new molecules with potential antithrombotic activities (Bigalke et al., 2010). GPVI is of central importance for the activation of platelets by fibrillar collagen of types I and III, which is abundantly present in atherosclerotic plaques. In vitro studies of platelet thrombus formation under flow on immobilized plaque extracts supported a crucial role for GPVI in platelet accumulation on atherosclerotic lesions (Cosemans et al., 2005; Reininger et al., 2010). Moreover, GPVI deficiency prevented thrombus formation on injured plaques in apolipoprotein E [(ApoE)(−/−) mice (Kuijpers et al., 2009; Hechler and Gachet, 2011)]. In vivo, recombinant soluble GPVI was shown to accumulate within atherosclerotic plaques in rabbits and to protect ApoE(−/−) mice from arterial remodeling after mechanical

This work was supported by the Institut National de la Santé et de la Recherche Médicale, the Fondation de France [Grant 2007001960]; the Agence National de la Recherche [Grant 07EPMB-002-01]; and the Seventh Framework Programme of the European Comission [Grant 260309]. C.T. is supported by postdoctoral fellowship from the French Chinese Foundation for Science and Applications.

C.G. and M.J.-P. contributed equally to this work.

Article, publication date, and citation information can be found at http://jpet.aspetjournals.org.

http://dx.doi.org/10.1124/jpet.111.189050.

[S] The online version of this article (available at http://jpet.aspetjournals.org) contains supplemental material.

ABBREVIATIONS: GPVI, glycoprotein VI; ApoE, apolipoprotein E; CRP, collagen-related peptide; $DIOC_6$, 3,3′-dihexyloxacarbocyanine iodide; ES, embryonic stem; FITC, fluorescein isothiocyanate; hGPVI, human glycoprotein VI; MFI, mean fluorescence intensity; mGPVI, mouse glycoprotein VI; PCR, polymerase chain reaction; WT, wild-type; SV40, simian virus 40.

injury (Schönberger et al., 2008). It is noteworthy that targeting GPVI appears to carry a low bleeding risk. Thus, patients presenting a congenital (Dumont et al., 2009) or autoimmune GPVI deficiency display a mild bleeding phenotype (Sugiyama et al., 1987; Nurden et al., 2009). Furthermore, GPVI expression being restricted to platelets and megakaryocytes, the side effects of GPVI antagonists should be limited (Jandrot-Perrus et al., 2000).

Several strategies may be employed to inhibit GPVI-triggered platelet activation. Use of the soluble immunoadhesin GPVI-Fc to compete for collagen binding (Jandrot-Perrus et al., 2000) has been reported to reduce thrombosis in different animal models, limit plaque development in hypercholesterolemic rabbits, and inhibit neointima formation after plaque denudation in ApoE(−/−) mice (Massberg et al., 2004; Schönberger et al., 2008). Very recently, a phase I study demonstrated that GPVI-Fc efficiently inhibited collagen-induced platelet aggregation with no alteration of primary hemostasis (Ungerer et al., 2011). A second possibility is the use of antibodies directed against GPVI, because some of them have the capacity to block the interaction of GPVI with collagen (Lecut et al., 2003; Smethurst et al., 2004), whereas others induce platelet GPVI depletion (Takayama et al., 2008).

Despite accumulating data in favor of GPVI as a major target, controversies subsist when considering the different mouse models of thrombosis. Depending on the model used to induce thrombosis, the respective parts played by GPVI and thrombin in mediating thrombus growth may vary. GPVI seems to be important in mechanical injury models (Massberg et al., 2004; Bender et al., 2011) but less as the involvement of thrombin increases (Mangin et al., 2006; Hechler et al., 2010). The only clear-cut result yet obtained in mice is the absence of bleeding when GPVI is absent or blocked.

Mice are obviously not entirely satisfactory for preclinical studies, also due to sequence differences in several domains of GPVI, which could influence collagen-induced responses. Alignment of the human GPVI (hGPVI) and mouse GPVI (mGPVI) sequences shows 64.4% identity for the amino acids and 67.3% for the nucleotide sequences; the intracellular domain of mGPVI is 24 residues shorter than that of hGPVI (Jandrot-Perrus et al., 2000). The extracellular domains of GPVI are not identical between species, and most of the blocking antibodies directed against hGPVI do not bind to mGPVI (Lecut et al., 2003; Smethurst et al., 2004).

Thus, to be able to evaluate the antithrombotic potentials of compounds targeting human GPVI, we have constructed a mouse model humanized for GPVI to be subjected to various models of arterial thrombosis. We report here that these mice are viable and fertile and exhibit normal functional responses to all of the agonists tested. The blocking antibody Fab fragment 9O12.2 directed against human GPVI inhibits collagen-induced platelet aggregation in vitro and ex vivo and limits thrombosis in vivo. Hence, these mice represent a model that could be used in preclinical studies to screen anti-GPVI agents. In addition, they should allow for better investigation of the relevance of targeting GPVI in various models of thrombosis including stroke and thrombosis at sites of atherosclerotic plaque rupture.

Materials and Methods

Materials. The monoclonal antibodies to human GPVI, 3J24.2 and 9O12.2, were obtained by immunization with GPVI-Fc. 9O12.2 recognizes human but not mGPVI (Lecut et al., 2003) (Supplemental Materials and Methods).

Generation of hGPVI Mice. The *gp6* knockin mutant mouse line was established at the Mouse Clinical Institute (Illkirch, France; http://www-mci.u-strasbg.fr). The *gp6* gene contains eight exons and is localized on chromosome 19q13 in human and on chromosome 7 in mouse. Constructs were designed to knockin the mouse *gp6* gene by introducing the sequence of the human *gp6* gene into exon 1 at ATG (Fig. 1A). The targeting vector was constructed as follows: the homologous 5′ (4.1 kb) and 3′ (3.4 kb) arms were amplified by polymerase chain reaction (PCR) using bacterial artificial chromosome (bMQ461E17) DNA as a template and subcloned into a Mouse Clinical Institute proprietary vector, resulting in the step 1 plasmid. This Mouse Clinical Institute vector has a floxed neomycin resistance cassette. A 1.2-kb fragment corresponding to the human *gp6* gene (GenBank accession number XM_145298) followed by a simian virus 40 (SV40) polyA sequence to stop transcription was amplified by PCR and subcloned into the step 1 plasmid to generate the final targeting construct. The linearized construct was electroporated into

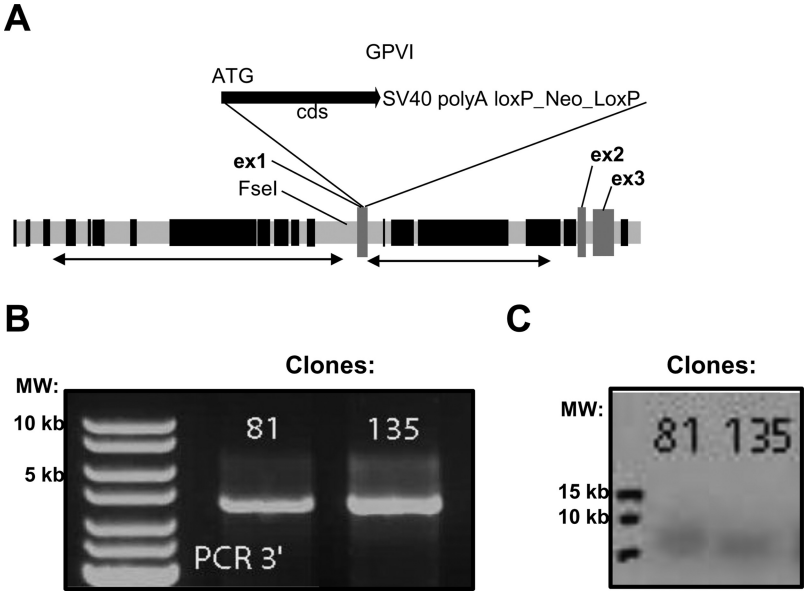

Fig. 1. Generation and characterization of mice expressing hGPVI. A, a targeting vector was designed to replace the mouse *gp6* gene with the human gene. The human *gp6* sequence followed by a SV40 polyA domain and a LoxP-flanked neomycin cassette was inserted at the ATG position of the mouse *gp6* gene. B and C, the presence of the vector in electroporated ES cells was confirmed by PCR (B) and Southern blot analysis (C).

129S2/SvPas mouse embryonic stem (ES) cells. After selection, the targeted clones were identified by PCR using external primers and further confirmed by Southern blot analysis with 5′ and 3′ external probes. Two positive ES clones were injected into C57BL/6J blastocytes, and the male chimeras derived gave germline transmission. The neomycin resistance cassette was removed by crossing the chimeras with mice expressing Flp recombinase. Heterozygous knockin mice were intercrossed, and human GPVI mouse lines were established at the animal facilities of the Etablissement Français du Sang-Alsace. Genotyping was performed on mouse tail DNA by PCR. Because mice were not backcrossed, littermates were used throughout the studies as controls for the knockin mice. All of the procedures for animal experiments were performed in accordance with the directives of the European Parliament and the Council on the Protection of Animals Used for Scientific Purposes as defined by European laws.

Platelet Preparation and Aggregation, Expression of Platelet Glycoproteins, Integrin $\alpha_{IIb}\beta_3$ Activation, and P-Selectin Exposure. Murine platelets were obtained, and platelet aggregation was analyzed as reported previously. Surface expression of the main glycoproteins and the number of hGPVI copies on hGPVI mouse platelets were determined by flow cytometry.

Platelet Count and Size. Whole blood was collected into EDTA (6 mM) after severing the mouse tail. The platelet count and size were determined in a scil Vet abc automatic cell counter (Scil Animal Care Company, Holtzheim, France) set to murine parameters.

In Vitro Flow-Based Adhesion Assay. Thrombus growth was observed in real time by flowing hirudinated whole blood labeled with 3,3′-dihexyloxacarbocyanine iodide ($DIOC_6$) into rectangular glass microcapillaries coated with type I fibrillar collagen.

Tail Bleeding Time. The tail bleeding time was measured as described previously (Léon et al., 2007). The time required for the arrest of bleeding and blood loss were recorded.

Thromboembolism Model. The model of systemic vascular thromboembolism induced by the infusion of a collagen (0.3 mg/kg)/adrenaline (60 μg/kg) mixture has been described previously (DiMinno and Silver, 1983).

Arterial Thrombosis Models. Anesthetized mice received an injection of $DIOC_6$ to label platelets. Superficial and deep laser-induced mesenteric thrombosis was investigated as described previously (Hechler et al., 2010). Mechanically induced thrombosis was obtained by the compression of the aorta with a forceps for 60 s. Thrombus formation was monitored in real time with a fluorescence

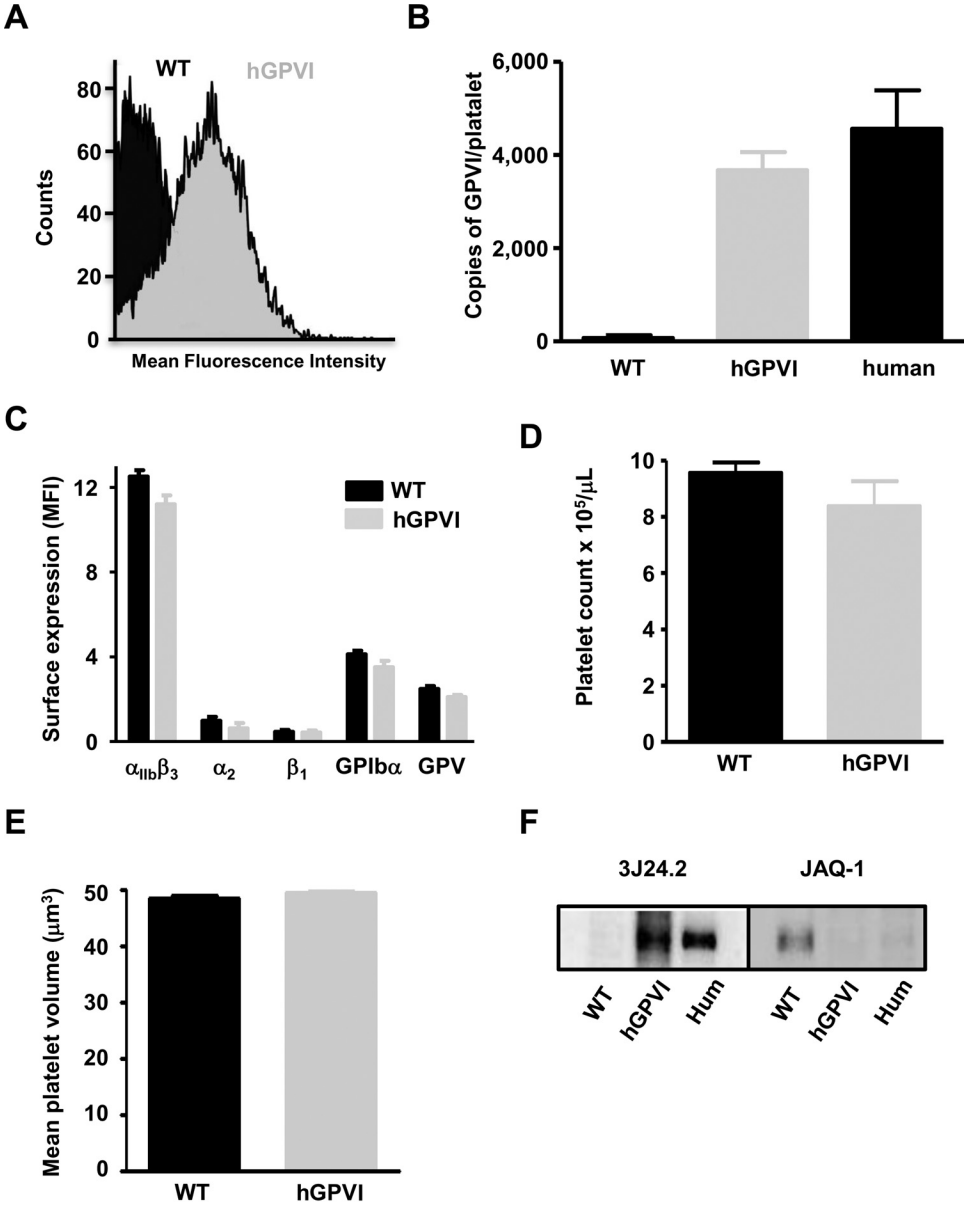

Fig. 2. Hematological parameters and platelet properties in hGPVI mice. A, surface expression of hGPVI on platelets from hGPVI mice and WT littermates was determined by flow cytometry using the anti-GPVI antibody 3J24.2. The histogram is representative of three separate experiments. B, quantification of hGPVI copies on WT (n = 6), hGPVI (n = 6), and human platelets (n = 3). Values represent the mean ± S.E.M. C, surface expression of various glycoproteins on platelets from hGPVI mice and WT littermates. Results are expressed as the mean fluorescence intensity (MFI) ± S.E.M. in three platelet preparations for each group of mice. D, platelet counts. Values represent the mean ± S.E.M. (n = 3) in hGPVI and WT mice. E, platelet volume. Values represent the mean platelet volume ± S.E.M. (n = 3) in blood from hGPVI mice and WT littermates. F, whole platelet lysates from hGPVI mice, WT littermates, or human volunteers were immunoblotted with 3J24.2 or JAQ1 and revealed with a secondary anti-human or anti-mouse antibody, respectively.

microscope coupled to a charge-coupled device camera, and analyses were performed with surface quantification software.

Statistical Analysis. All of the values are reported as the mean ± S.E.M. unless otherwise indicated. Data were compared by two-tailed paired Student's *t* tests, and differences were considered to be significant for $p < 0.05$. For thromboembolism experiments, analyses were performed with a log-rank test. All of the tests were carried out using Prism software (GraphPad Software Inc., San Diego, CA). [Detailed methods are accessible in the Supplemental Materials and Methods.]

Results

Generation of Mice Expressing hGPVI in Their Platelets. To generate mice expressing hGPVI, a vector containing the full-length cDNA sequence of *hgp6* followed by a SV40 polyA domain and a LoxP-flanked neomycin cassette, used for selection, was inserted into the *mgp6* gene at the ATG position (Fig. 1A). The targeting vectors were electroporated into ES cells. Screening by PCR (Fig. 1B) and Southern blot analysis (Fig. 1C) identified two positive clones for injection into blastocytes. Animals with germline transmission were obtained, and heterozygotes were intercrossed.

Normal Hematological Parameters and Platelet Properties and Function in hGPVI Mice. No obvious developmental or morphological abnormalities were observed in hGPVI mice. The knockin mouse platelets expressed the human form of GPVI at their surface, as could be demonstrated by flow cytometry using the selective antibody 3J24.2 (Fig. 2A). The number of human GPVI copies was 3673 ± 390 at the surface of hGPVI mouse platelets as compared with 4560 ± 827 for human platelets ($p > 0.05$; $n = 3$) (Fig. 2B). The expression of prominent platelet surface glycoproteins, including integrins $\alpha_{IIb}\beta_3$, α_2, β_1, glycoprotein (GP)Ibα, and glycoprotein (GP)V, was normal in hGPVI mice ($n = 6$–12) (Fig. 2C). In addition, platelet counts and size were unchanged in hGPVI mice (838 ± 89 × 10^3/μl; 49.3 ± 0.3 μm^3) as compared with littermates (956 ± 38 × 10^3/μl; 48.3 ± 0.7 μm^3) ($p > 0.05$; $n = 3$) (Fig. 2, D and E). Immunoblots of platelet lysates using the anti-human GPVI monoclonal antibody 3J24.2 indicated that the GPVI expressed by hGPVI mouse platelets migrated with a molecular mass of 58 kDa under nonreducing conditions, in agreement with the mass of human GPVI (Fig. 2F). Immunoblots with the anti-mGPVI monoclonal antibody JAQ1 confirmed the absence of the expression of mGPVI in the platelets of hGPVI mice (Fig. 2F).

Normal Platelet Functional Responses in hGPVI Mice. The rates and amplitudes of hGPVI platelet aggregation were normal in response to various agonists, including collagen (1 μg/ml), U46619 (2 μM), the protease-activated receptor 4 agonist peptide AYPGKF (500 μM), thrombin (0.5 U/ml), and ADP (5 μM) ($n = 2$) (Fig. 3A). No anomalies of fibrinogen binding were observed in hGPVI mice upon stimulation with ADP (2 μM), AYPGKF (1 mM), thrombin (0.25 U/ml), or collagen-related peptide (CRP) (0.5 μg/ml) ($n = 5$) (Fig. 3B). P-Selectin exposure was also normal in response to AYPGKF (1 mM), thrombin (0.25 U/ml), or CRP (0.5 μg/ml) ($n = 5$) (Fig. 3C). These results indicate that replacing mGPVI with hGPVI did not alter the functional responses of platelets to their main agonists.

9O12.2 Binds to hGPVI Platelets and Inhibits Collagen- and CRP-Induced Platelet Activation and Aggregation. We first showed by flow cytometry that 9O12.2 Fab

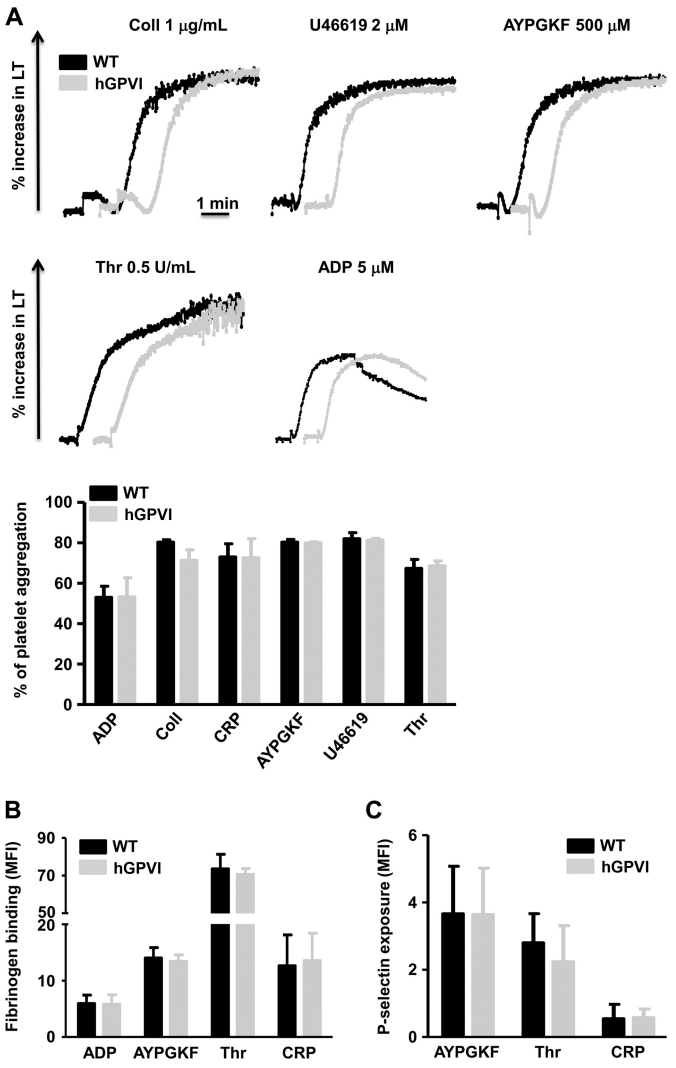

Fig. 3. Normal aggregation responses, fibrinogen binding, and P-selectin exposure in hGPVI platelets. A, washed platelets (3.0 × 10^8/ml) from hGPVI mice and WT littermates were stimulated with collagen (1 μg/ml), U46619 (2 μM), AYPGKF (500 μM), and ADP (5 μM) in the presence of fibrinogen (64 μg/ml) or with thrombin (0.5 U/ml) in the absence of fibrinogen. Aggregation profiles are representative of three separate experiments. The bar graph represents the percentage of platelet aggregation at 3 min ($n = 3$). B and C, washed platelets (5.0 × 10^7/ml) from hGPVI mice and WT littermates were stimulated for 10 min with ADP (2 μM), AYPGKF (1 mM), thrombin (0.25 U/ml), or CRP-XL (1 μg/ml), and the binding of Alexa Fluor 488-fibrinogen (B) or a fluorescein isothiocyanate (FITC)-anti-P-selectin antibody (C) was detected by flow cytometry. Results represent the geometric mean of the relative fluorescence intensity ± S.E.M. in five separate experiments performed in duplicate.

effectively binds to hGPVI platelets, whereas this was not the case for wild-type (WT) platelets (data not shown). In vitro, a concentration of 50 μg/ml 9O12.2, as used previously for nonhuman primate (cynomolgus) platelets (Ohlmann et al., 2008), markedly impaired collagen- (0.25 μg/ml) and CRP-induced (1 μg/ml) platelet aggregation. At a higher collagen concentration (1 μg/ml), the aggregation was delayed, and the lag phase was prolonged. In contrast, 9O12.2 had no effect on stimulation with ADP (2 μM), U46619 (2 μM), AYPGKF (500 μM), or thrombin (0.5 U/ml) ($n = 3$) (Fig. 4A). The 9O12.2 Fab fragment also prevented CRP-induced fibrinogen binding ($p < 0.05$; $n = 3$), whereas no reduction was observed in response to ADP, AYPGKF, or thrombin (Fig.

4B). In addition, we observed 62% inhibition of platelet aggregation ($p < 0.05$; $n = 7$) when hGPVI mouse whole blood pretreated with 9O12.2 (50 μg/ml) was perfused at 1500 s^{-1} over collagen (Fig. 4C). These results indicate that 9O12.2 efficiently blocks GPVI of hGPVI mouse platelets and that this animal model therefore should be suitable for ex vivo and in vivo studies.

Ex Vivo Effects of 9O12.2. On the basis of previous studies in cynomolgus monkeys, a dose of 4 mg/kg 9O12.2 Fab was injected into hGPVI mice to evaluate its effects ex vivo (Ohlmann et al., 2008). We confirmed by flow cytometry that 9O12.2 efficiently bound circulating platelets. The binding was maximal 30 min postinjection before progressively decreasing to become undetectable at 24 h ($n = 6$) (Fig. 5A). We also checked that after the injection of 9O12.2 collagen-induced platelet aggregation was delayed in platelet-rich plasma ($n = 3$) (Fig. 5B). Whole blood collected from hGPVI mice 30 min after the injection of 9O12.2 displayed a 71% decrease in platelet aggregate formation when perfused at 1500 s^{-1} over collagen, indicating that this agent was able to block GPVI ex vivo (area under the curve; $p < 0.05$; control Fab, $n = 3$; 9O12.2 Fab, $n = 4$) (Fig. 5C). 9O12.2 did not induce thrombocytopenia postinjection ($n = 5$) (data not shown). GPVI expression was apparently decreased by 30% ($p < 0.05$; $n = 5$) 30 min after the injection of 9O12.2, possibly due to steric hindrance related to 9O12.2 binding, and returned to normal after 330 min ($p > 0.05$; $n = 5$) (Fig. 5D).

9O12.2 Does Not Impair Hemostasis. The effect of 9O12.2 on hemostasis was evaluated 30 min postinjection in a tail bleeding assay. The hGPVI mice injected with 4 or 8 mg/kg 9O12.2 showed no prolongation of the tail bleeding time when compared with control ($p > 0.05$) (Fig. 5E). Moreover, 9O12.2 did not increase the volume of blood lost (25 ± 21 μl at 4 mg/kg and 18 ± 6 μl at 8 mg/kg) as compared with a control Fab (29 ± 17 μl) ($p > 0.05$; $n = 6$) (Fig. 5F). These results suggest that blockade of GPVI preserves normal hemostatic properties despite decreased platelet aggregation in response to collagen.

Effects of 9O12.2 on Thrombus Formation In Vivo. The effects of 9O12.2 in hGPVI mice first were evaluated in a model of platelet-dependent intravascular thrombosis induced by a collagen/adrenaline mixture. Injection of the control Fab led to no reduction in vascular thrombosis, with 100% mortality within 3 min ($n = 5$). In contrast, hGPVI mice

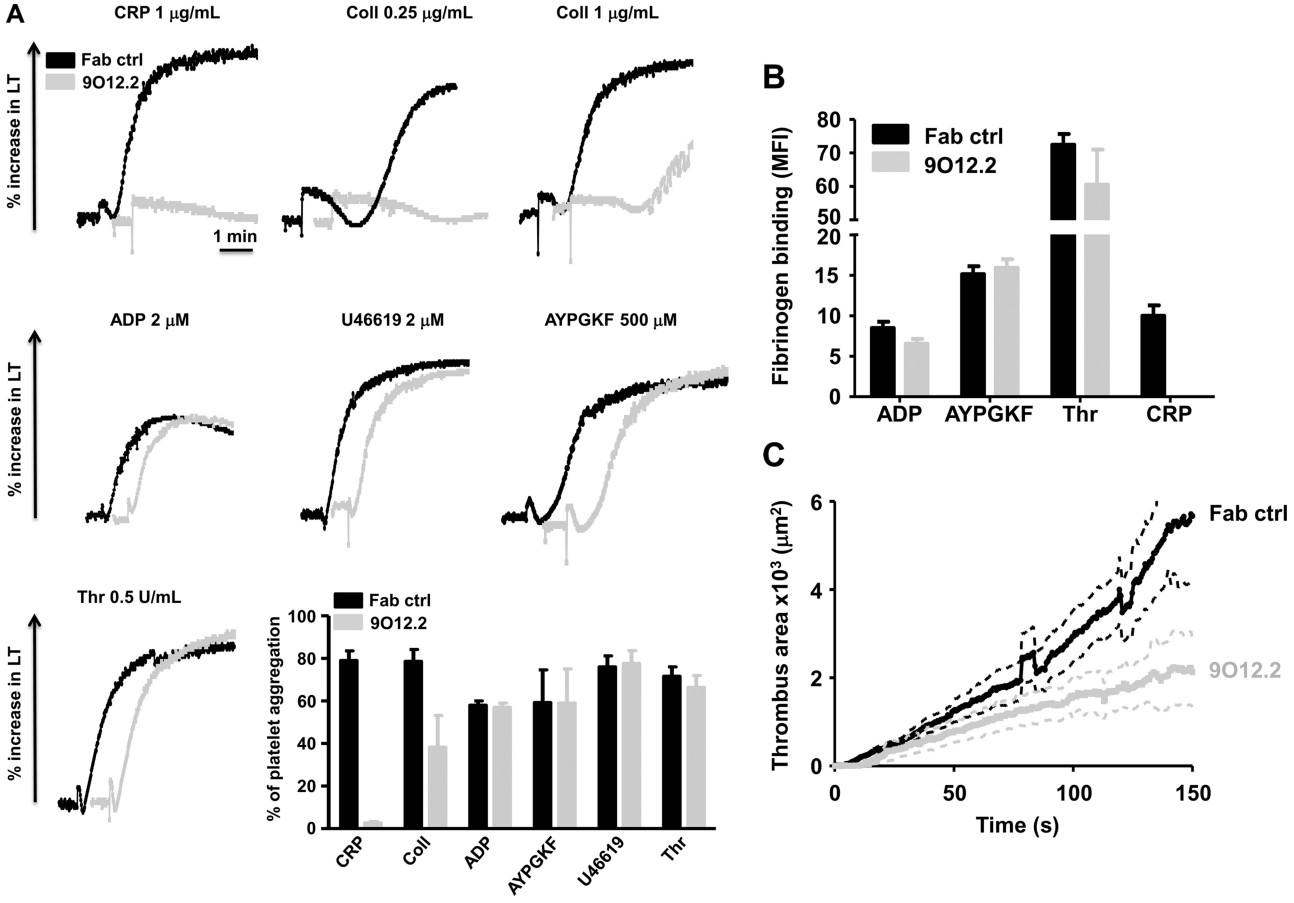

Fig. 4. In vitro effects of 9O12.2 Fab on platelet aggregation and fibrinogen binding. A, washed hGPVI platelets (3.0×10^8/ml) were incubated with 50 μg/ml control or 9O12.2 Fab and stimulated with collagen (0.25 or 1 μg/ml), CRP (1 μg/ml), ADP (2 μM), U46619 (2 μM), and AYPGKF (500 μM) in the presence of fibrinogen (64 μg/ml) or with thrombin (0.5 U/ml) in the absence of fibrinogen. Aggregation profiles are representative of three separate experiments. The bar graph represents the percentage of platelet aggregation at 3 min ($n = 3$); Coll, 1 μg/ml. B, washed hGPVI platelets (5.0×10^7/ml) were incubated with 50 μg/ml control or 9O12.2 Fab and stimulated for 10 min with ADP (2 μM), AYPGKF (1 mM), thrombin (0.25 U/ml), or CRP-XL (1 μg/ml) and analyzed for the binding of Alexa Fluor 488-fibrinogen. Results represent the geometric mean of the relative fluorescence intensity ± S.E.M. in three separate experiments performed in duplicate. C, anticoagulated whole blood (hirudin 100 U/ml) from hGPVI mice was labeled with FITC-RAM.1 (5 μg/ml) and incubated with 50 μg/ml control or 9O12.2 Fab for 10 min before being perfused over collagen for 150 s at 1500 s^{-1}. Platelet aggregation was visualized in real time under an inverted fluorescence microscope, and the calculated thrombus area represents the mean fluorescence intensity (MFI) ± S.E.M. in seven independent perfusions.

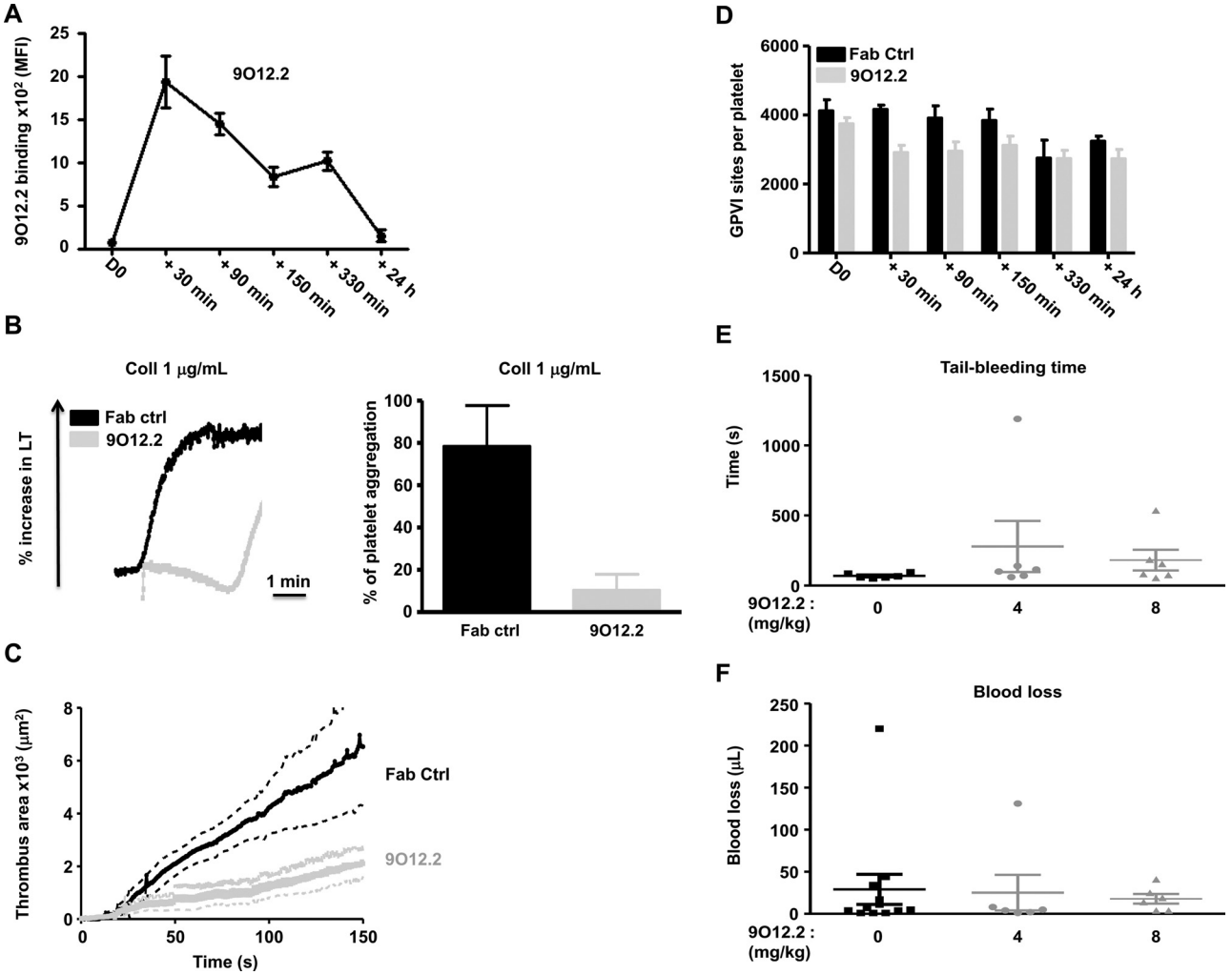

Fig. 5. Effect of a bolus injection of 9O12.2 Fab into hGPVI mice. Control or 9O12.2 Fab (4 mg/kg) was injected retro-orbitally into hGPVI mice. A, platelet-bound 9O12.2 Fab was quantified by flow cytometry using a FITC-conjugated anti-mouse antibody. Results are expressed as the MFI ± S.E.M. in six different platelet preparations. B, platelet-rich plasma from hGPVI mice (3.0×10^8/ml) was stimulated with collagen (1 µg/ml) for 50 min postinjection of 9O12.2. The aggregation profile is representative of three separate experiments. The bar graph represents the percentage of collagen-induced platelet aggregation at 3 min ($n = 3$). C, anticoagulated whole blood (hirudin 100 U/ml) from hGPVI mice was labeled with FITC-RAM.1 (5 µg/ml) and perfused over collagen for 150 s at 1500 s^{-1}. Platelet aggregation was visualized in real time, and the calculated thrombus area represents the MFI ± S.E.M. in three and four independent perfusions. D, hGPVI was quantified using 3J24.2, an anti-hGPVI monoclonal antibody, and a FITC-conjugated specific anti-mouse Fc antibody. Values represent the MFI ± S.E.M. in mice injected with control or 9O12.2 Fab ($n = 6$). E and F, tail bleeding times (E) and volumes of blood lost over a period of 30 min (F) were measured in groups of six hGPVI mice treated with control Fab or 9O12.2 Fab at 4 or 8 mg/kg. Symbols represent individual mice: mean value ± S.E.M. for each population is indicated.

injected with 4 mg/kg 9O12.2 had a lower death rate, with three of five mice still being alive 30 min after collagen/adrenaline challenge, and 100% of them survived when a higher concentration of 8 mg/kg was used ($p < 0.05$; $n = 5$) (Fig. 6A). A laser-injury thrombosis model was then used to evaluate the influence of 9O12.2 on localized thrombus formation in hpg6 mice. Mice treated with 9O12.2 Fab (4 mg/kg) ($n = 17$ in six mice) but not those receiving the control Fab displayed a 44% decrease ($p < 0.05$; $n = 16$ in six mice) in thrombus formation after superficial laser injury of mesenteric arterioles (Fig. 6B). As expected, 9O12.2 did not protect hGPVI mice against thrombosis after deep laser injury, a model reported previously to generate significant amounts of thrombin (Mangin et al., 2006; Hechler et al., 2010) (Fig. 6C). However, when thrombin was blocked with hirudin in the same model, the role of GPVI in thrombus growth was unmasked, with 9O12.2 further inhibiting residual thrombosis (43% reduction; $p < 0.05$; $n = 6$) (Fig. 6D). Finally, the 9O12.2 Fab fragment also protected hGPVI mice against thrombosis after forceps induced-mechanical injury of the aorta, with a 48% reduction (area under the curve; $p < 0.05$; control Fab, $n = 5$; 9O12.2 Fab, $n = 6$) in thrombus size as compared with that of controls (Fig. 6E). Overall, these data indicate that hGPVI mice are a suitable tool to evaluate the role of human GPVI in various models of thrombosis and to screen anti-GPVI compounds.

Discussion

In this study, we successfully introduced the human *gp6* gene into the corresponding mouse locus, with resultant expression of human GPVI at appropriate levels (~3700 copies) and extinction of the expression of murine GPVI, in the absence of any other modifications of platelet morphology, counts, or function

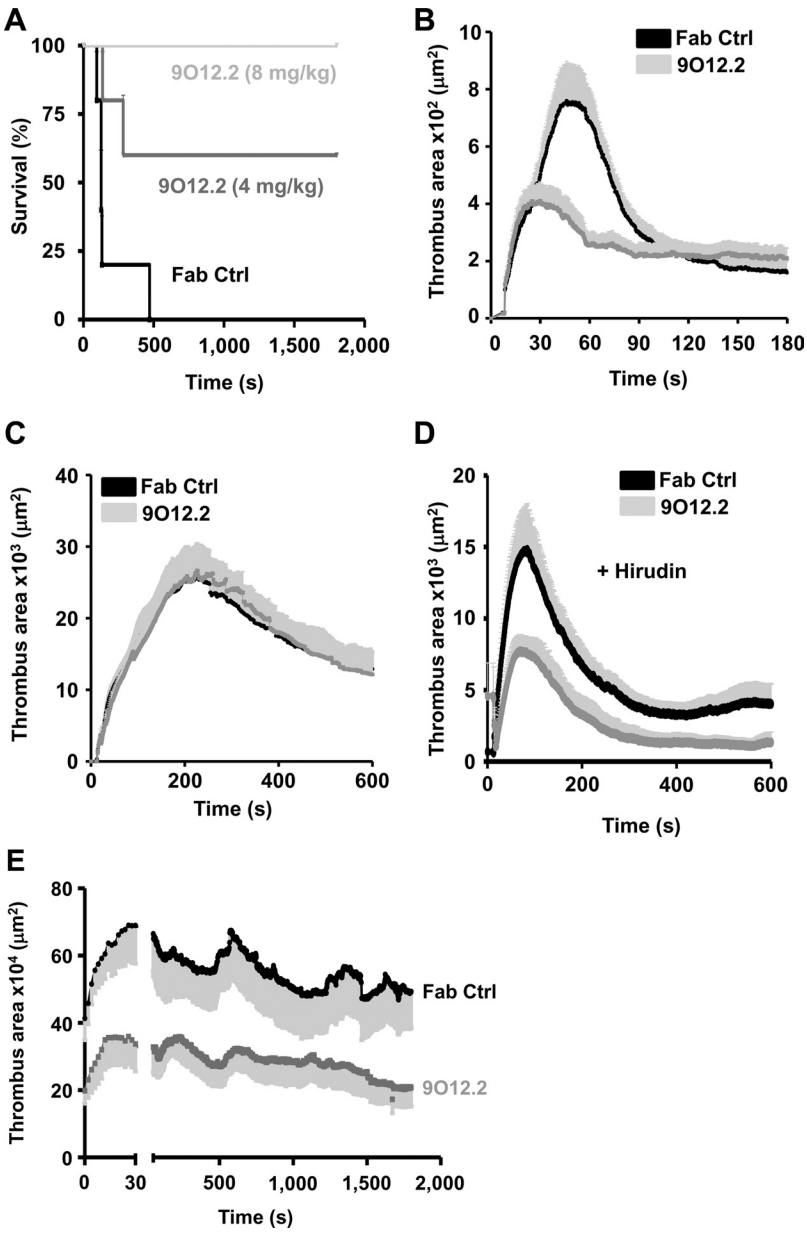

Fig. 6. Effect of 9O12.2 Fab on in vivo thrombus formation in hGPVI mice. A–E, control or 9O12.2 Fab (4 or 8 mg/kg) and $DIOC_6$ (5 µl of a 100 µM solution per gram of body weight) was injected into the jugular vein of hGPVI mice; 30 min postinjection, the mice were subjected to three thrombosis models. A, systemic thromboembolism was induced by the infusion of a collagen/adrenaline mixture. Results are expressed as the percentage survival as a function of time; $n = 5$ mice in each group. Superficial (B) or deep (C and D) laser-induced lesions were generated in the mesenteric arteries. B, superficial injury. Control, $n = 17$ vessels in six mice; 9O12.2 Fab, $n = 16$ vessels in six mice. C, deep injury. Control, $n = 8$ vessels in six mice; 9O12.2 Fab, $n = 7$ vessels in six mice. D, deep injury after treatment with hirudin (10 mg/kg subcutaneously). Control Fab, $n = 7$ vessels in four mice; 9O12.2 Fab, $n = 6$ vessels in three mice. E, a mechanical injury was produced in the aorta of mice with forceps. Control Fab, $n = 5$; 9O12.2 Fab, $n = 6$. B–E, tracings represent the mean surface area ± S.E.M. of the thrombi developing over time.

(Best et al., 2003). The specific anti-human GPVI blocking Fab 9O12.2 selectively inhibited GPVI-mediated responses without impairing those mediated by other receptors. Injection of 9O12.2 into hGPVI animals did not impair hemostasis but significantly reduced systemic and localized arterial thrombosis.

Injection of 9O12.2 did not result in a thrombocytopenic phenotype, in agreement with the data obtained in monkeys (Ohlmann et al., 2008). This contrasts with the effects of other anti-GPVI antibodies, notably JAQ1, which is known to induce transient thrombocytopenia accompanied by total and long-lasting deletion of GPVI from the platelet surface. GPVI down-regulation occurs through receptor internalization and clearing or ectodomain shedding and is coupled to distinct signaling pathways downstream of the FcRγ-immunoreceptor tyrosine-based activation motif (Rabie et al., 2007). This mechanism is assumed to be responsible for the GPVI deficiencies observed in patients presenting anti-GPVI autoantibodies (Sugiyama et al., 1987; Nurden et al., 2009). In contrast, 9O12.2 has a very limited effect, if any, probably because it is devoid of activating properties and hence not able to induce the signals required for internalization (Lecut et al., 2003).

After one bolus injection of 9O12.2 Fab, ex vivo collagen-induced platelet aggregation was delayed, thus confirming that the occupancy of GPVI by the antibody impairs the binding of the receptor to collagen. This inhibited thrombus growth when whole blood was perfused over collagen at arterial shear rates (Fig. 5C).

The mouse model developed here allowed us to evaluate in vivo the effects of an antiplatelet agent targeting hGPVI, whereas to date this was only possible in vitro (Lecut et al., 2003) and ex vivo (Ohlmann et al., 2008; Ungerer et al., 2011). 9O12.2 protected hGPVI mice against lethal thromboembolism, a model sensitive to the antiplatelet agents clopidogrel targeting $P2Y_{12}$ and tirofiban blocking integrin $\alpha_{IIb}\beta_3$ (Supplemental Fig. 1A). In addition, 9O12.2 had an antithrombotic effect after superficial laser injury of mesenteric arterioles, which formed a thrombus that can be inhibited by

$P2Y_{12}$ and integrin $\alpha_{IIb}\beta_3$ blockers (Nonne et al., 2005; Hechler et al., 2010). 9O12.2 also prevented thrombus growth after deep laser injury under conditions where thrombin was blocked. These results are consistent with those obtained in mice deficient in or immunodepleted of GPVI (Mangin et al., 2006; Hechler et al., 2010). Finally, 9O12.2 provided protection against thrombosis after mechanical injury of the aorta, a model that is sensitive to aspirin and clopidogrel (Supplemental Fig. 1B). This result is in agreement with previously published data (Bender et al., 2011). Thus, inhibition of hGPVI in a murine context resulted in a similar reduction in thrombosis as that afforded by the invalidation or immunodepletion of mGPVI. This hGPVI mouse model is thus suitable to determine the in vivo efficacy of a blocking anti-GPVI Fab or any other agent targeting GPVI. Furthermore, our model opens up the new and unique perspective of evaluating the antithrombotic effects of anti-GPVI compounds in diseased vessels, to mimic as closely as possible the pathological conditions leading to atherothrombosis. This is currently under investigation, with the generation by bone marrow transplantation of chimeric mice deficient in ApoE and having hGPVI platelets that will be subjected to our recently described models of thrombosis (Hechler and Gachet, 2011).

Concerning the bleeding risk, we found that the injection of 9O12.2 into hGPVI mice did not prolong the tail bleeding time or increase the blood loss. Our observation is in agreement with a recent phase I study in which healthy volunteers treated with the soluble dimeric GPVI-Fc fusion protein Revacept displayed unaltered bleeding time (Ungerer et al., 2011). The hGPVI model therefore offers the possibility of establishing the bleeding tendency of anti-GPVI compounds alone or associated with dual or triple therapy with other antiplatelet agents.

In conclusion, we describe here a unique animal model that permits the in vivo evaluation of agents targeting hGPVI in terms of efficacy and safety. In particular, this model can predict the response to anti-GPVI agents in human more accurately than conventional mouse models. This should enable the determination of doses and therapeutic combinations, thus providing an important preclinical tool, which may help to design future clinical studies.

Acknowledgments

We thank François Lanza for helpful discussion, Nicolas Receveur and Stéphanie Magnenat for technical assistance, and Juliette Mulvihill for editorial help.

Authorship Contributions

Participated in research design: Mangin, Gachet, and Jandrot-Perrus.

Conducted experiments: Mangin, Tang, Bourdon, Loyau, Freund, and Hechler.

Performed data analysis: Mangin, Tang, Bourdon, Loyau, Hechler, and Gachet.

Wrote or contributed to the writing of the manuscript: Mangin, Hechler, Gachet, and Jandrot-Perrus.

References

Bender M, Hagedorn I, and Nieswandt B (2011) Genetic and antibody-induced glycoprotein VI deficiency equally protects mice from mechanically and FeCl(3)-induced thrombosis. *J Thromb Haemost* **9:**1423–1426.

Best D, Senis YA, Jarvis GE, Eagleton HJ, Roberts DJ, Saito T, Jung SM, Moroi M, Harrison P, Green FR, et al. (2003) GPVI levels in platelets: relationship to platelet function at high shear. *Blood* **102:**2811–2818.

Bigalke B, Krämer BF, Seizer P, Fateh-Moghadam S, Gawaz M, and Lindemann S (2010) Diagnostic and therapeutic potentials of platelet glycoprotein VI. *Semin Thromb Hemost* **36:**203–211.

Cosemans JM, Kuijpers MJ, Lecut C, Loubele ST, Heeneman S, Jandrot-Perrus M, and Heemskerk JW (2005) Contribution of platelet glycoprotein VI to the thrombogenic effect of collagens in fibrous atherosclerotic lesions. *Atherosclerosis* **181:** 19–27.

DiMinno G and Silver MJ (1983) Mouse antithrombotic assay: a simple method for the evaluation of antithrombotic agents in vivo. Potentiation of antithrombotic activity by ethyl alcohol. *J Pharmacol Exp Ther* **225:**57–60.

Dumont B, Lasne D, Rothschild C, Bouabdelli M, Ollivier V, Oudin C, Ajzenberg N, Grandchamp B, and Jandrot-Perrus M (2009) Absence of collagen-induced platelet activation caused by compound heterozygous GPVI mutations. *Blood* **114:**1900–1903.

Hechler B and Gachet C (2011) Comparison of two murine models of thrombosis induced by atherosclerotic plaque injury. *Thromb Haemost* **105 (Suppl 1):**S3–S12.

Hechler B, Nonne C, Eckly A, Magnenat S, Rinckel JY, Denis CV, Freund M, Cazenave JP, Lanza F, and Gachet C (2010) Arterial thrombosis: relevance of a model with two levels of severity assessed by histologic, ultrastructural and functional characterization. *J Thromb Haemost* **8:**173–184.

Jackson SP and Schoenwaelder SM (2003) Antiplatelet therapy: in search of the 'magic bullet.' *Nat Rev Drug Discov* **2:**775–789.

Jandrot-Perrus M, Busfield S, Lagrue AH, Xiong X, Debili N, Chickering T, Le Couedic JP, Goodearl A, Dussault B, Fraser C, et al. (2000) Cloning, characterization, and functional studies of human and mouse glycoprotein VI: a platelet-specific collagen receptor from the immunoglobulin superfamily. *Blood* **96:**1798–1807.

Kuijpers MJ, Gilio K, Reitsma S, Nergiz-Unal R, Prinzen L, Heeneman S, Lutgens E, van Zandvoort MA, Nieswandt B, Egbrink MG, et al. (2009) Complementary roles of platelets and coagulation in thrombus formation on plaques acutely ruptured by targeted ultrasound treatment: a novel intravital model. *J Thromb Haemost* **7:**152–161.

Lecut C, Feeney LA, Kingsbury G, Hopkins J, Lanza F, Gachet C, Villeval JL, and Jandrot-Perrus M (2003) Human platelet glycoprotein VI function is antagonized by monoclonal antibody-derived Fab fragments. *J Thromb Haemost* **1:**2653–2662.

Léon C, Eckly A, Hechler B, Aleil B, Freund M, Ravanat C, Jourdain M, Nonne C, Weber J, Tiedt R, et al. (2007) Megakaryocyte-restricted MYH9 inactivation dramatically affects hemostasis while preserving platelet aggregation and secretion. *Blood* **110:**3183–3191.

Mangin P, Yap CL, Nonne C, Sturgeon SA, Goncalves I, Yuan Y, Schoenwaelder SM, Wright CE, Lanza F, and Jackson SP (2006) Thrombin overcomes the thrombosis defect associated with platelet GPVI/FcRgamma deficiency. *Blood* **107:**4346–4353.

Massberg S, Konrad I, Bültmann A, Schulz C, Münch G, Peluso M, Lorenz M, Schneider S, Besta F, Müller I, et al. (2004) Soluble glycoprotein VI dimer inhibits platelet adhesion and aggregation to the injured vessel wall in vivo. *FASEB J* **18:**397–399.

Nonne C, Lenain N, Hechler B, Mangin P, Cazenave JP, Gachet C, and Lanza F (2005) Importance of platelet phospholipase Cgamma2 signaling in arterial thrombosis as a function of lesion severity. *Arterioscler Thromb Vasc Biol* **25:**1293–1298.

Nurden P, Tandon N, Takizawa H, Couzi L, Morel D, Fiore M, Pillois X, Loyau S, Jandrot-Perrus M, and Nurden AT (2009) An acquired inhibitor to the GPVI platelet collagen receptor in a patient with lupus nephritis. *J Thromb Haemost* **7:**1541–1549.

Ohlmann P, Hechler B, Ravanat C, Loyau S, Herrenschmidt N, Wanert F, Jandrot-Perrus M, and Gachet C (2008) Ex vivo inhibition of thrombus formation by an anti-glycoprotein VI Fab fragment in non-human primates without modification of glycoprotein VI expression. *J Thromb Haemost* **6:**1003–1011.

Rabie T, Varga-Szabo D, Bender M, Pozgaj R, Lanza F, Saito T, Watson SP, and Nieswandt B (2007) Diverging signaling events control the pathway of GPVI down-regulation in vivo. *Blood* **110:**529–535.

Reininger AJ, Bernlochner I, Penz SM, Ravanat C, Smethurst P, Farndale RW, Gachet C, Brandl R, and Siess W (2010) A 2-step mechanism of arterial thrombus formation induced by human atherosclerotic plaques. *J Am Coll Cardiol* **55:**1147–1158.

Schönberger T, Siegel-Axel D, Bussl R, Richter S, Judenhofer MS, Haubner R, Reischl G, Klingel K, Münch G, Seizer P, et al. (2008) The immunoadhesin glycoprotein VI-Fc regulates arterial remodelling after mechanical injury in $ApoE^{-/-}$ mice. *Cardiovasc Res* **80:**131–137.

Smethurst PA, Joutsi-Korhonen L, O'Connor MN, Wilson E, Jennings NS, Garner SF, Zhang Y, Knight CG, Dafforn TR, Buckle A, et al. (2004) Identification of the primary collagen-binding surface on human glycoprotein VI by site-directed mutagenesis and by a blocking phage antibody. *Blood* **103:**903–911.

Sugiyama T, Okuma M, Ushikubi F, Sensaki S, Kanaji K, and Uchino H (1987) A novel platelet aggregating factor found in a patient with defective collagen-induced platelet aggregation and autoimmune thrombocytopenia. *Blood* **69:**1712–1720.

Takayama H, Hosaka Y, Nakayama K, Shirakawa K, Naitoh K, Matsusue T, Shinozaki M, Honda M, Yatagai Y, Kawahara T, et al. (2008) A novel antiplatelet antibody therapy that induces cAMP-dependent endocytosis of the GPVI/Fc receptor gamma-chain complex. *J Clin Invest* **118:**1785–1795.

Ungerer M, Rosport K, Bültmann A, Piechatzek R, Uhland K, Schlieper P, Gawaz M, and Münch G (2011) Novel antiplatelet drug revacept (Dimeric Glycoprotein VI-Fc) specifically and efficiently inhibited collagen-induced platelet aggregation without affecting general hemostasis in humans. *Circulation* **123:**1891–1899.

Yousuf O and Bhatt DL (2011) The evolution of antiplatelet therapy in cardiovascular disease. *Nat Rev Cardiol* **8:** 547–559.

Address correspondence to: Dr. Christian Gachet, Unité Mixte de Recherche Scientifique 949, Institut National de la Santé et de la Recherche Médicale, Université de Strasbourg, Etablissement Français du Sang-Alsace, 10 Rue Spielmann, BP 36, F-67065 Strasbourg Cedex, France. E-mail: christian.gachet@efs-alsace.fr